

See discussions, stats, and author profiles for this publication at: <https://www.researchgate.net/publication/51904504>

# High H-2 Uptake in Li-, Na-, K-Metalated Covalent Organic Frameworks and Metal Organic Frameworks at 298 K

ARTICLE in THE JOURNAL OF PHYSICAL CHEMISTRY A · DECEMBER 2011

Impact Factor: 2.69 · DOI: 10.1021/jp206981d · Source: PubMed

---

CITATIONS

17

READS

100

## 3 AUTHORS:



[Jose L. Mendoza-Cortes](#)

Florida State University

15 PUBLICATIONS 2,183 CITATIONS

[SEE PROFILE](#)



[Sang Soo Han](#)

Korea Research Institute of Standards and S...

58 PUBLICATIONS 1,900 CITATIONS

[SEE PROFILE](#)



[William A. Goddard](#)

California Institute of Technology

1,337 PUBLICATIONS 68,337 CITATIONS

[SEE PROFILE](#)

# High H<sub>2</sub> Uptake in Li-, Na-, K-Metalated Covalent Organic Frameworks and Metal Organic Frameworks at 298 K

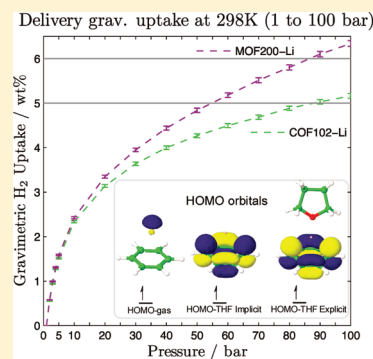
José L. Mendoza-Cortés,<sup>†</sup> Sang Soo Han,<sup>‡</sup> and William A. Goddard, III<sup>\*,†</sup>

<sup>†</sup>Materials and Process Simulation Center, California Institute of Technology, Pasadena, California 91106, United States

<sup>‡</sup>Center for Nanocharacterization, Korea Research Institute of Standards and Science, Daejeon 305-340, Republic of Korea

 Supporting Information

**ABSTRACT:** The Yaghi laboratory has developed porous covalent organic frameworks (COFs), COF102, COF103, and COF202, and metal–organic frameworks (MOFs), MOF177, MOF180, MOF200, MOF205, and MOF210, with ultrahigh porosity and outstanding H<sub>2</sub> storage properties at 77 K. Using grand canonical Monte Carlo (GCMC) simulations with our recently developed first principles based force field (FF) from accurate quantum mechanics (QM), we calculated the molecular hydrogen (H<sub>2</sub>) uptake at 298 K for these systems, including the uptake for Li-, Na-, and K-metallated systems. We report the total, delivery and excess amount in gravimetric and volumetric units for all these compounds. For the gravimetric delivery amount from 1 to 100 bar, we find that eleven of these compounds reach the 2010 DOE target of 4.5 wt % at 298 K. The best of these compounds are MOF200-Li (6.34) and MOF200-Na (5.94), both reaching the 2015 DOE target of 5.5 wt % at 298 K. Among the undoped systems, we find that MOF200 gives a delivery amount as high as 3.24 wt % while MOF210 gives 2.90 wt % both from 1 to 100 bar and 298 K. However, none of these compounds reach the volumetric 2010 DOE target of 28 g H<sub>2</sub>/L. The best volumetric performance is for COF102-Na (24.9), COF102-Li (23.8), COF103-Na (22.8), and COF103-Li (21.7), all using delivery g H<sub>2</sub>/L units for 1–100 bar. These are the highest volumetric molecular hydrogen uptakes for a porous material under these thermodynamic conditions. Thus, one can obtain outstanding H<sub>2</sub> uptakes with Li, Na, and K doping of simple frameworks constructed from simple, cheap organic linkers. We present suggestions for strategies for synthesis of alkali metal-doped MOFs or COFs.



## 1. INTRODUCTION

A current major obstacle to molecular hydrogen (H<sub>2</sub>) as an alternative source of energy is the difficulty of storage at operational temperatures. The U.S. Department of Energy (DOE) has set the 2010 targets of 4.5 wt % and 28 g/L at room temperature (and 5.5 wt % and 40 g/L for 2015).<sup>1,2</sup> Many materials have been proposed that might approach these demanding goals. Chemisorption of H<sub>2</sub> in solid systems can lead to the required capacities; however chemisorption generally leads to interaction energies that are too strong (>30 kJ/mol) compounded by additional barriers that lead to very slow kinetics. On the other hand, physisorption generally has good kinetics (no barrier), but the net bonding is too weak (interaction energy <10 kJ/mol) for substantial storage at room temperature.<sup>3</sup> The discovery of robust microporous covalent organic frameworks (COFs)<sup>4–6</sup> and metal–organic frameworks (MOFs)<sup>7–9</sup> have brought excitement that these systems might lead to a solution to this problem due to their (1) high surface area: MOF210 has the world record in Brunauer–Emmett–Teller (BET) surface area of 6240 m<sup>2</sup>/g, and Langmuir surface area of 10400 m<sup>2</sup>/g;<sup>9</sup> (2) low density: 0.17 g/cm<sup>3</sup> for COF108, the lowest for a crystalline material,<sup>5</sup> while 0.22 g/cm<sup>3</sup> for MOF200;<sup>9</sup> and (3) high porosity:

as high as 3.59 cm<sup>3</sup>/g for MOF200, 3.60 cm<sup>3</sup>/g for MOF210, 1.81 for COF102 and 2.05 for COF103.

However, these compounds show a poor uptake of H<sub>2</sub> at room temperature due to the weak interactions between the frameworks and H<sub>2</sub>. As a way to obtain higher interaction energies we proposed metallating MOFs, such as MOF5<sup>10</sup> and MOF177,<sup>11</sup> with Li and we showed that this could increase the uptake sufficiently to achieve up to 5.5 wt % excess H<sub>2</sub> at 300 K.<sup>10</sup>

In the current study, we report the excess and delivery sorption curve from 1 to 100 bar at room temperature for the latest generation of MOF and COFs, including the Li-, Na-, and K-metallated analogs. We also calculate the thermodynamics for the formation of the alkaline species in the gas phase and in tetrahydrofuran (THF), including the possibility of clustering and adducts (Li–benzene vs Li–Li), to explore the plausibility for the experimental synthesis under room temperature. We then propose that metallating the new COFs and MOFs with alkali metals (Li, Na, and K) can dramatically increase the binding energy and, thus, the H<sub>2</sub> uptake.

**Received:** July 21, 2011

**Revised:** December 16, 2011

**Published:** December 21, 2011

**Table 1. Properties of the Frameworks Used in This Work: Surface Area ( $S_A$ ), Pore Volume ( $V_p$ ), and Density ( $\rho$ )<sup>a</sup>**

material	$S_A, \text{m}^2 \text{ g}^{-1}$	$V_p, \text{cm}^3 \text{ g}^{-1}$	$\rho, \text{g cm}^{-3}$	material	$S_A, \text{m}^2 \text{ g}^{-1}$	$V_p, \text{cm}^3 \text{ g}^{-1}$	$\rho, \text{g cm}^{-3}$
COF102	4940	1.81	0.42	COF102-Na	4930	1.35	0.50
COF103	5230	2.05	0.38	COF103-Na	5090	1.54	0.46
COF202	4500	1.37	0.54	COF202-Na	3950	1.09	0.59
MOF177	4800 (4500)	1.93 (1.89)	0.43	MOF177-Na	4710	1.49	0.46
MOF180	5940	3.50	0.25	MOF180-Na	6010	2.92	0.28
MOF200	5730 (4530)	4.04 (3.59)	0.22	MOF200-Na	6020	3.17	0.26
MOF205	4630 (4460)	2.21 (2.16)	0.38	MOF205-Na	4950	1.75	0.44
MOF210	5570 (6240)	3.61 (3.60)	0.25	MOF210-Na	5610	3.05	0.28
COF102-Li	5360	1.65	0.44	COF102-K	4380	1.10	0.56
COF103-Li	5500	1.85	0.38	COF103-K	4800	1.27	0.52
COF202-Li	4250	1.25	0.54	COF202-K	3570	0.94	0.64
MOF177-Li	5100	1.74	0.39	MOF177-K	4220	1.27	0.51
MOF180-Li	6440	3.26	0.26	MOF180-K	5630	2.60	0.31
MOF200-Li	6480	3.69	0.23	MOF200-K	5600	2.73	0.29
MOF205-Li	5270	2.00	0.40	MOF205-K	4340	1.50	0.49
MOF210-Li	6130	3.39	0.26	MOF210-K	5140	2.73	0.31

<sup>a</sup>The values in parentheses were reported in the literature.<sup>9</sup>  $S_A$  and  $V_p$  were estimated from rolling an Ar molecule with a diameter of 3.42 Å<sup>19</sup> over the framework's surface.

For this study, we used FF parameters developed from accurate quantum mechanics (CCSD(T) and MP2) for describing the physisorption of H<sub>2</sub> onto the alkali–aromatic complex adducts. We then used GCMC based on this first principles FF to calculate the loading curves of H<sub>2</sub> versus pressure at room temperature. These simulations demonstrate that the metalated versions of these materials can achieve the major DOE gravimetric targets for 2010 and even 2015. We report H<sub>2</sub> uptake using total, delivery, and excess units resulting from metalating the highest surface areas (SA) and the highest pore volume ( $V_p$ ) frameworks with Li, Na, or K, as well as the pristine analogs. This includes the latest generation of COFs (COF102, COF103, and COF202) and MOFs (MOF177, MOF180, MOF200, MOF205, and MOF210), which physical properties are summarized in Table 1.

## 2. COMPUTATIONAL DETAILS

**2.1. Quantum Mechanics Calculations and Development of the Parameters for Nonbond Interactions.** To develop FF parameters for the nonbonded interactions between H<sub>2</sub> and MOF/COFs, we used DFT/M06<sup>12</sup> with the 6-31G\*\*++ basis set calculations as implemented in Jaguar<sup>13</sup> to determine the locations and numbers of Li, Na, or K atoms on the aromatic linkers. We then used these geometries to calculate the binding energies from accurate quantum mechanical methods (CCSD(T) and MP2) which are capable of accurately describing the London dispersion forces. The FF were then fitted to these QM energies and geometries.

We use the Morse potential (eq 1), which we found to describe well the nonbond interaction of H<sub>2</sub>. The Morse function involves three parameters: the well depth  $D$ , the equilibrium bond distance  $r_0$ , and the stiffness  $\alpha$ .

$$U_{ij}^{\text{Morse}}(r_{ij}) = D \left\{ e^{\alpha(1 - r_{ij}/r_0)} - 2e^{\alpha/2(1 - r_{ij}/r_0)} \right\} \quad (1)$$

Our experience is that the Morse function gives a slightly better description than exponential-6, which performs much better than

**Table 2. Nonbonded FF Parameters Used for This Study Based on MP2 for Li and CCSD(T) for Na and K<sup>a</sup>**

term	$D, \text{kJ mol}^{-1}$	$r_0, \text{\AA}$	$\alpha$
H <sub>H2</sub> –H <sub>H2</sub>	$7.60 \times 10^{-2}$	3.57	10.7
H <sub>H2</sub> –C <sub>COF/MOF</sub>	$4.22 \times 10^{-1}$	3.12	12.0
H <sub>H2</sub> –H <sub>COF/MOF</sub>	$3.63 \times 10^{-3}$	3.25	12.0
H <sub>H2</sub> –Zn <sub>COF/MOF</sub>	$5.21 \times 10^{-1}$	2.76	13.4
H <sub>H2</sub> –O <sub>COF/MOF</sub>	$1.05 \times 10^{-1}$	3.32	12.0
H <sub>H2</sub> –B <sub>COF/MOF</sub>	$2.02 \times 10^{-1}$	3.49	10.6
H <sub>H2</sub> –Si <sub>COF/MOF</sub>	$4.61 \times 10^{-1}$	3.53	14.2
H <sub>H2</sub> –Li <sub>COF/MOF</sub>	9.03	2.02	7.13
H <sub>H2</sub> –Na <sub>COF/MOF</sub>	5.73	2.49	7.71
H <sub>H2</sub> –K <sub>COF/MOF</sub>	2.71	3.13	8.04

<sup>a</sup>The function form (Morse) is given in eq 1.  $D$  is the well depth,  $r_0$  is the equilibrium bond distance, and  $\alpha$  determines the force constant.<sup>10,16,17</sup>

Lennard-Jones 12–6 potential.<sup>14,15</sup> Table 2 shows the parameters used for this work.<sup>10,16,17</sup>

**2.2. Valence Bond Force Field.** The equilibrium structures of the pristine MOFs and COFs used in this study were optimized with the Dreiding force field<sup>18</sup> starting with the reported experimental structures. We have shown that the resulting structures are in very good agreement with experiment.<sup>10,11</sup> The coordinates of the optimized metalated structures are shown in the Supporting Information.

**2.3. Grand Canonical Monte Carlo Loading Curves.** We used the first principles based force field described above in grand canonical Monte Carlo (GCMC) ensemble simulations. Here for each temperature and pressure, we constructed 3,000,000 configurations to compute the average loading for which we observed convergence was obtained. Every GCMC step allows four possible events, translation, rotation, creation, and annihilation, each at equal probability. We used the GCMC code as implemented in Cerius2. The structures of the optimized frameworks are shown in Figure 1.

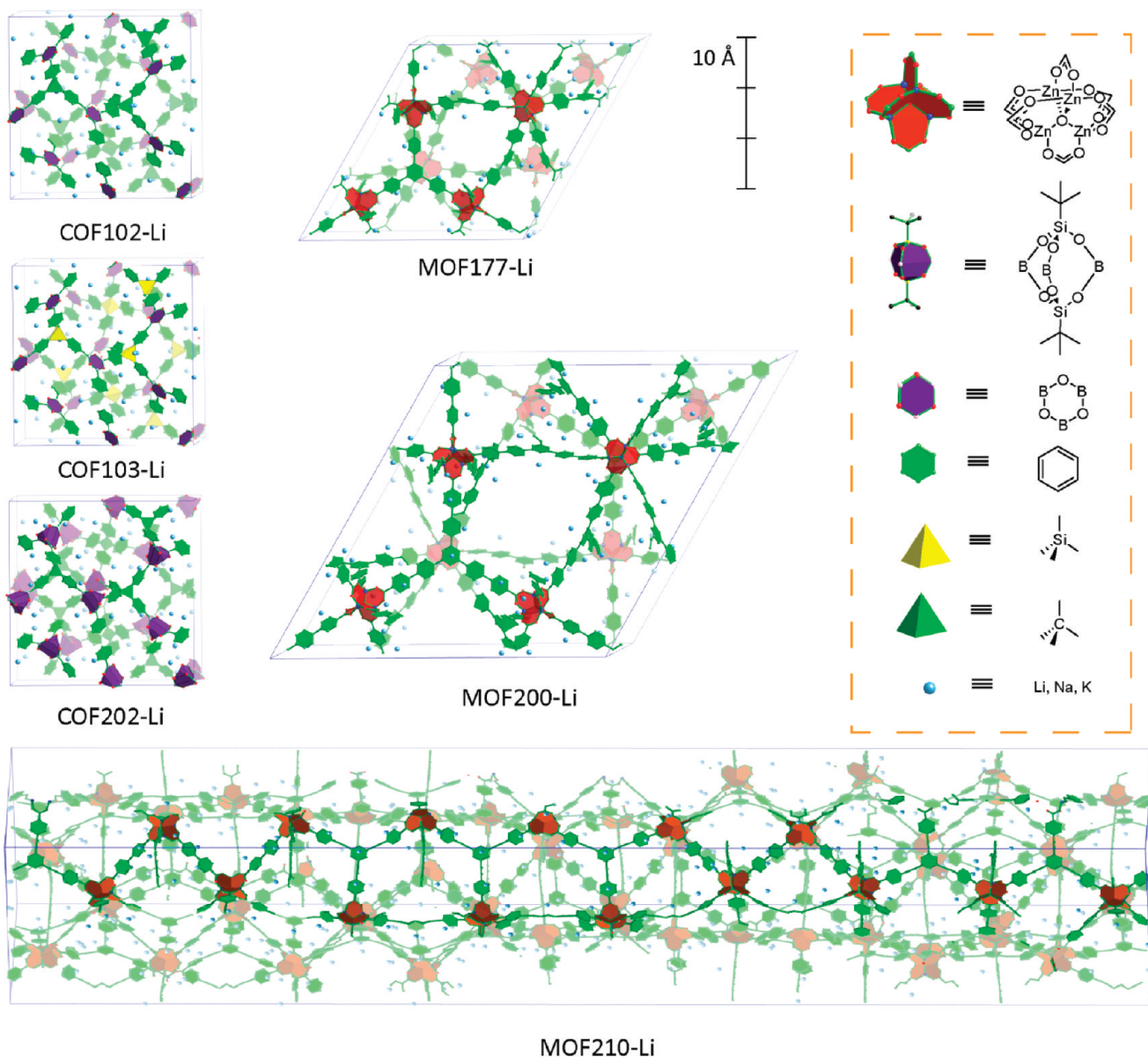


**Figure 1.** Structures of the Li-doped COFs and MOFs studied in this work. Hydrogen atoms have been omitted for clarity.

### 3. RESULTS AND DISCUSSION

**3.1. Nature of the Chemical Bond for the Li–Benzene (Li–Bz) Systems.** To investigate the plausibility on the formation of Li–Bz adduct, we calculated their thermodynamics from quantum mechanics in the gas phase and in tetrahydrofuran (THF). Nonperiodic QM calculations were carried out using the B3LYP<sup>20,21</sup> and M06<sup>12</sup> hybrid DFT functionals with the Jaguar code.<sup>13</sup> Here we used the 6-31G\*\*++ and 6-311G\*\*++ basis sets. All geometries were optimized using the analytic Hessian to determine that the local minima have no negative curvatures (imaginary frequencies). The vibrational frequencies from the analytic Hessian were used to calculate the zero-point energy corrections at 0 K (Tables 3 and 4). To explore the solvation, we consider two different approaches explicit THF and implicit THF (for which we used the Poisson–Boltzmann continuum approximation; with  $\epsilon = 7.6$ ,  $R_0 = 2.52 \text{ \AA}$ ).<sup>22</sup> When we compared the binding energy for the Li–Li compounds, we found that M06 is closer than B3LYP to the

CCSD(T) calculations (Figure S1). The results for the thermodynamics at 298.15 K and 1.01 bar are shown in Figure 2. We observed that, in the gas phase, the Li–Bz is not thermodynamically favorable; however, MO6 predicts that the Li–Bz–Li compound is favorable in the gas phase with respect to Li(g) and Bz(g). This observation prompted us to calculate the thermodynamics in THF since this might help to stabilize the polarized Li species and, therefore, have a favorable thermodynamics under these conditions. As predicted, we can see from Figure 2, if we are able to form Li(g) as well as Bz(g) and dissolve them in THF, we will observe the formation of Li–Bz adduct is thermodynamically favorable ( $\Delta G = -22.4 \text{ kcal/mol}$ ). Although such an experimental setup might be difficult, a good approximation could be attained by dissolving Li(s) and Bz(l) in THF at very low concentrations. On the other hand, Tacke<sup>23</sup> has shown experimentally and theoretically that when concentrated quantities of Bz and Li in THF are used at 77 K; C–H activation occurs and Li–Ph + Li–H compounds are formed. In a related work, they also showed that the formation

**Table 3.** Electronic Energy for the Optimized Systems Using Different Basis Sets (6-31G\*\*++ and 6-311G\*\*++) and Different Functionals (M06 and B3LYP) are Presented<sup>a</sup>

compound	M06/6-31G**++		M06/6-311G**++		B3LYP/6-31G**++		B3LYP/6-311G**++	
	$E_{SCF}$ (kcal mol <sup>-1</sup> )	BSSE (kcal mol <sup>-1</sup> )	$E_{SCF}$ (kcal mol <sup>-1</sup> )	BSSE (kcal mol <sup>-1</sup> )	$E_{SCF}$ (kcal mol <sup>-1</sup> )	BSSE (kcal mol <sup>-1</sup> )	$E_{SCF}$ (kcal mol <sup>-1</sup> )	BSSE (kcal mol <sup>-1</sup> )
1Li	-4696.9	N/A	-4696.8	N/A	-4700.7	N/A	-4700.9	N/A
2Li	-9416.2	0.1	-9418.2	0.0	-9421.7	0.1	-9422.6	0.1
Bz	-145624.2	N/A	-145633.8	N/A	-145747.5	N/A	-145777.4	N/A
Li-Bz	-150323.8	0.3	-150353.6	0.3	-150449.1	0.4	-150479.6	0.5
Li-Bz-Li	-155032.6	1.1	-155066.2	0.9	-155153.2	0.7	-155188.3	0.5

<sup>a</sup>We also show the basis set superposition error (BSSE)<sup>35</sup> for the addition of a Li atom.

**Table 4.** Zero Point Energy (ZPE), Vibrational Enthalpy ( $H_{vib}$ ), Total Enthalpy ( $H_{tot}$ ), Vibrational Entropy ( $S_{vib}$ ), Total Entropy ( $S_{tot}$ ), and Solvation Energy ( $E_{solv}$ ) Obtained for the Different Compounds for 298.15 K<sup>a</sup>

compound	M06	B3LYP	M06		B3LYP		M06		B3LYP		M06	B3LYP
	ZPE (kcal mol <sup>-1</sup> )	ZPE (kcal mol <sup>-1</sup> )	$H_{vib}$ (kcal mol <sup>-1</sup> )	$H_{tot}$ (kcal mol <sup>-1</sup> )	$H_{vib}$ (kcal mol <sup>-1</sup> )	$H_{tot}$ (kcal mol <sup>-1</sup> )	$S_{vib}$ (kcal mol <sup>-1</sup> )	$S_{tot}$ (kcal mol <sup>-1</sup> )	$S_{vib}$ (kcal mol <sup>-1</sup> )	$S_{tot}$ (kcal mol <sup>-1</sup> )	$E_{solv}$ (kcal mol <sup>-1</sup> )	$E_{solv}$ (kcal mol <sup>-1</sup> )
1Li	0.0	0.0	0.0	1.5	0.0	1.5	0.0	33.9	0.0	33.9	0.0	0.0
2Li	0.5	0.5	0.2	2.3	0.2	2.3	1.2	47.2	1.2	47.2	0.0	0.0
Bz	62.8	63.1	1.0	3.4	1.0	3.3	4.5	64.2	4.4	64.1	-2.4	-2.3
Li-Bz	62.7	63.1	1.6	3.9	2.6	5.0	21.0	75.7	17.9	84.9	-19.6	-17.6
Li-Bz-Li	58.9	59.9	3.1	5.4	2.7	5.1	29.4	81.6	26.4	78.7	-35.8	-32.4

<sup>a</sup>ZPE energy corrections were obtained from the vibrational frequencies using the respective functional.

### Thermodynamics at 298.15 K and 1.00 atm

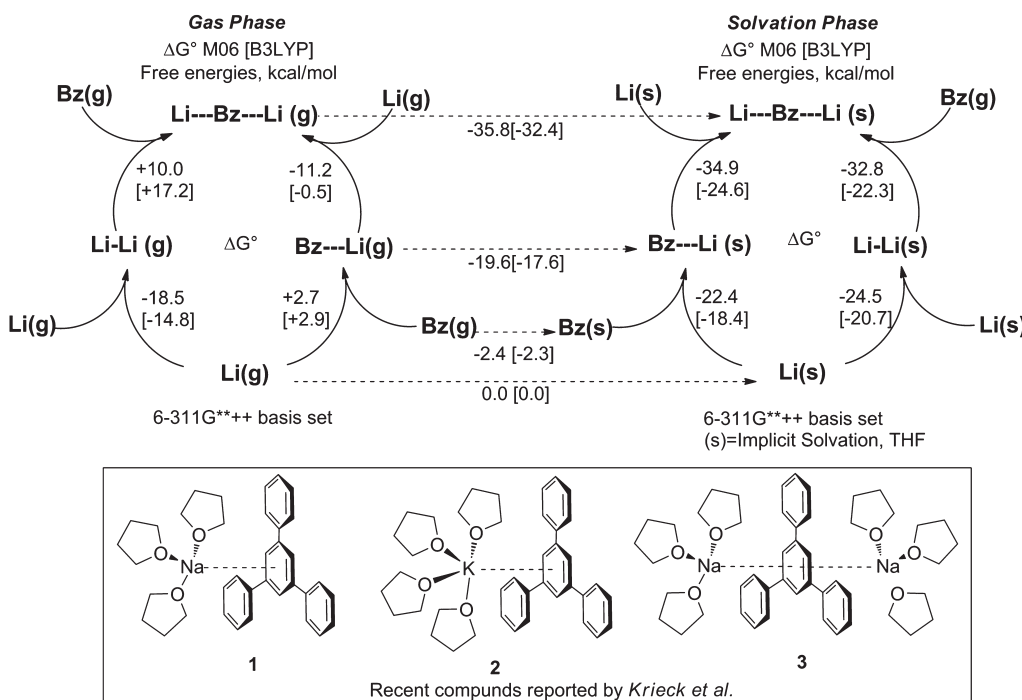


**Figure 2.** Calculations of the thermodynamics for the Li species were obtained using M06/6-311G\*\*++ and B3LYP/6-311G\*\*++. We defined the following quantities as  $g_{\text{gas}}G^{298\text{K}} = E_{SCF} + E_{ZPE} + H_{TOT} - T \times S_{TOT}$ , and  $solvG^{298\text{K}} = E_{SCF} + E_{SOLV} + E_{ZPE} + H_{VIB} + 6RT - T(0.5S_{VIB} + 0.5S_{TOT})$ . All the numerical data is shown in Tables 3 and 4. (Inset) 1, 2, and 3 are experimental compounds reported by Kriek et al.<sup>25</sup>

of R—Li···Bz adducts (R=H, CH<sub>3</sub>, and Ph) is possible when R—Li is used as the source for Li.<sup>24</sup> This suggests that the concentration of

Bz and Li, as well as the source of Li is key to obtain the structures here proposed and also confirms that Li clustering is not a major issue.

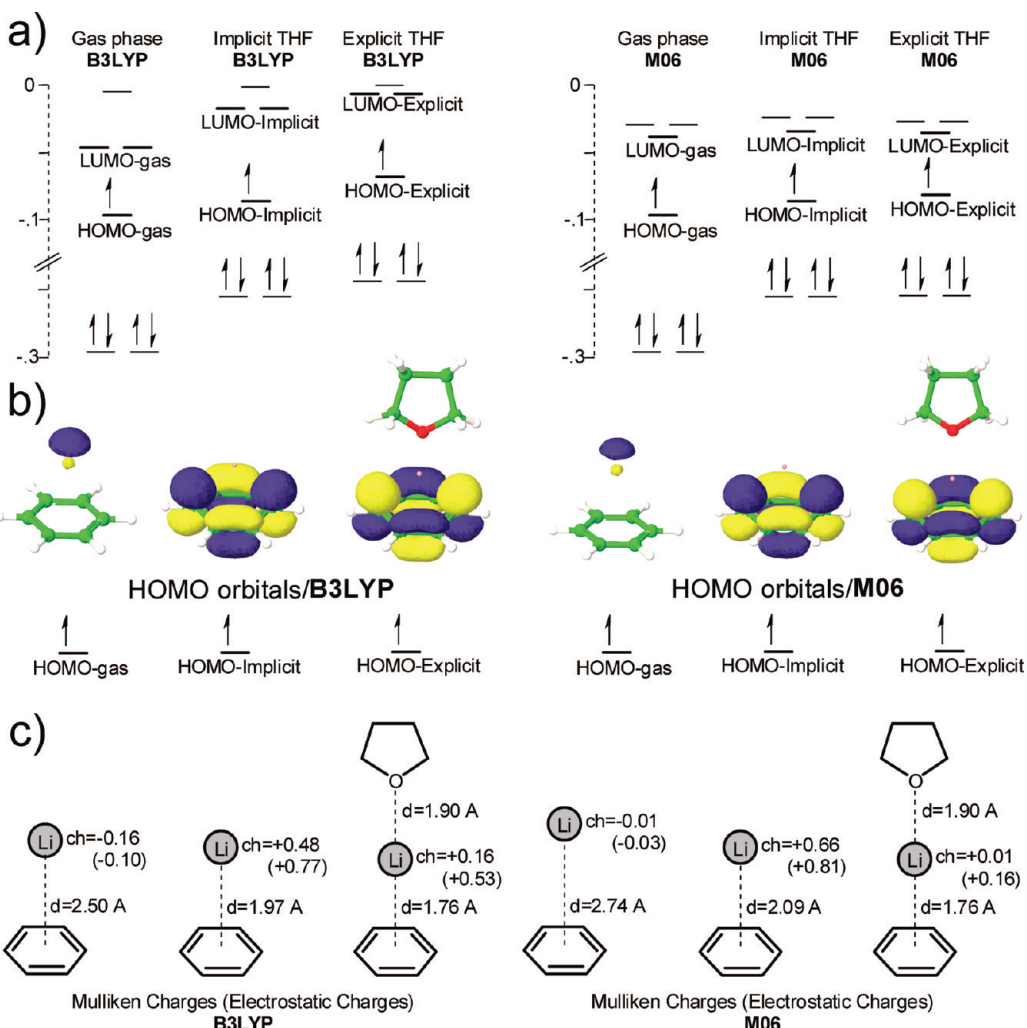


**Figure 3.** (a) Molecular orbital (MO) diagram for Li–Bz system. Units for the vertical axis are Hartrees. (b) Highest occupied molecular orbital (HOMO) for the Li–Bz for the gas phase, for the implicit THF and for explicit THF obtained from M06 and B3LYP. Atoms colors are C, green; H, white; and Li, pink. The colors of the orbitals yellow and dark blue represent an arbitrary positive and negative sign (c) Mulliken and electrostatic charges for Li–Bz (g), Li–Bz (implicit THF), and Li–Bz (explicit THF).

In a remarkable work, Kriek et al.<sup>25</sup> have been able to synthesized the  $(\text{THF})_3\text{Na}(\mu-\eta^6\text{-C}_6\text{H}_3\text{-2,4,6-Ph}_3)$  and  $(\text{THF})_4\text{K}(\mu-\eta^6\text{-C}_6\text{H}_3\text{-Ph}_3)$ , see inset of Figure 2. They were able to characterize these compounds by crystallography. This report shows that these systems can be synthesized but more remarkable it is the fact that the linkers used are the building blocks of MOF-177 and the precursor of MOF-200.

An interesting question to ask is where the electron goes once the Li–Bz adduct is formed. We calculated the HOMO and LUMO for these species and the results are shown in Figure 3. The molecular orbital diagram shows that the HOMO–LUMO gap narrows when THF is used (Figure 3a). The HOMO shows that the electron remains in the Li in the gas phase; however, if explicit or implicit THF is used, the electron is transferred the benzene ring (Figure 3b). This suggests that the transfer of electron is promoted by the solvent as expected.

A very important question for experimentalists is how to remove the THF from inside the structure in case it is strongly coordinate to the alkaline metal. The approach discussed so far uses an implicit model approximation (Poisson–Boltzmann continuum approximation) and this approach takes into account

the entire accessible surface area of the Li–Bz adduct but it does not consider explicit THF molecules for the calculation. Therefore, we have performed M06/6-311\*\*++ calculations to study how strongly the explicit oxygen of THF can coordinate with the Li from the Li–Bz adduct. We found that the free energy for this case is in the order of  $\Delta G = -1.0 \text{ kcal/mol}$  compared to the Li–Bz (implicit THF). Thus, if the THF is coordinated to the Li–Bz adduct, it can be removed. The M06 functional predicts that in gas phase the Li–Bz–Li would be stable while the Li–Bz would be unstable by  $\sim 2 \text{ kcal}$ . This is still within the level of accuracy for current DFT approach. However, B3LYP and M06 predict that 1 THF is necessary to stabilize the Bz–Li system if necessary.

A promising method to remove solvents from MOFs structures have been published by Hupp et al.<sup>26</sup> This method uses supercritical  $\text{CO}_2$  to activate the frameworks. They reported a spectacular 1200% uptake increase in some cases. This has been proven to lead to the successful activation in MOF-200, for example.<sup>9</sup> This method can be potentially used for the removal of THF since the molecules of THF are not strongly coordinated to the Li–Bz adduct as we have shown in our calculations.

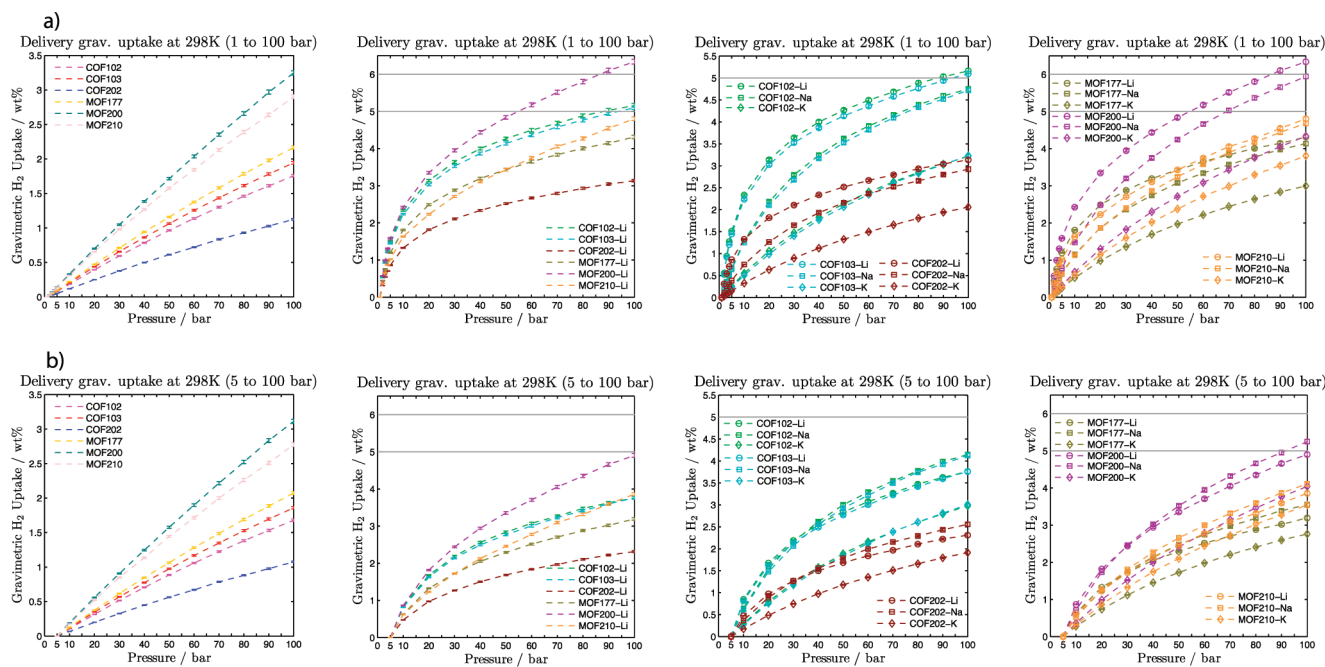


**Figure 4.** Delivery gravimetric uptake obtained for the studied COFs and MOFs, also the metalated analogs with Li, Na, and K are shown. MOF180 and MOF205 as well as the metalated cases are reported in the SI. In (a), we show the delivery amount using 1 bar as the basis, while in (b) we show the delivery amount using 5 bar as the basis. The error bars at each calculated point are shown, while on some cases they are too small to fit inside the symbols.

The supercritical CO<sub>2</sub> can be ultimately used to remove the most THF molecules and this approach could be tuned to avoid removing also the Li.

**3.2. Gravimetric Uptake.** We calculated the total wt% (see SI) gravimetric uptake of the frameworks at 298 K, which we used to estimate the *delivery* amount; this is the difference in the amount adsorbed at 100 bar versus a basis, say, 1 or 5 bar. The delivery amount is difficult to estimate experimentally;<sup>27,28</sup> however, it is very important for practical applications because it allows us to estimate the maximum amount that can be obtained if we unload the gas to, for example, ambient temperature and pressure.

Figure 4a shows the gravimetric delivery amount using 1 bar as the basis for pure and Li, Na, and K metalated COFs and MOFs. Here we see that the Li-metalated cases have a better performance than the Na-metalated cases, while Na-analogs lead to better performance than the K-cases. We can see that from 1 to 100 bar, 11 compounds reach an uptake higher than the 2010 DOE gravimetric target of 4.5 wt %: MOF200-Li (6.34), MOF200-Na (5.94), COF102-Li (5.16), MOF180-Li (5.16), MOF180-Na (4.91), MOF210-Li (4.80), COF103-Li (4.75), COF102-Na (4.75), COF103-Na (4.72), MOF210-Na (4.68), and MOF205-Li (4.58). From these compounds, only MOF200-Li and MOF200-Na reach an uptake over 5.5 wt % delivery. It is interesting to note that pure MOF200 gives a delivery amount as high as of 3.24 wt %, while MOF210 gives 2.90 wt % both at 100 bar and using 1 bar as the basis.

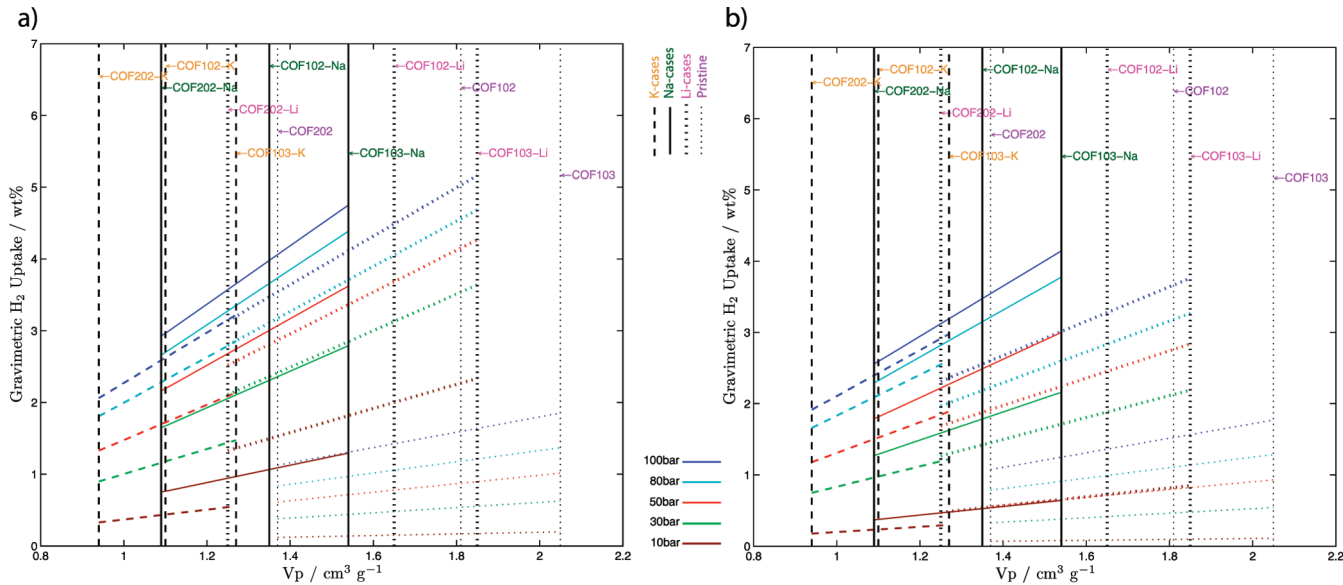
Figure 4b shows the gravimetric delivery amount using 5 bar as the basis at 298 K. Under these units, metalated cases lead to a different trend, with the uptake for Na-metalated > Li-metalated > K-metalated at pressures higher than 30 bar. Therefore, the best performance for gravimetric delivery (5–100 bar) is for MOF200-Na (5.25 wt %), followed by MOF200-Li (4.90 wt %), COF102-Na (4.75 wt %), COF103-Na (4.71 wt %), and

MOF210-Na (4.11 wt %). This shows another way to tune the properties to attain better delivery amounts for different basis (1 vs 5 bar). It is also worthwhile to highlight that, even with 5 bar as basis and 100 bar as the limit, pure MOF200 and pure MOF210 have a delivery amount of 3.11 and 2.77 wt %, respectively.

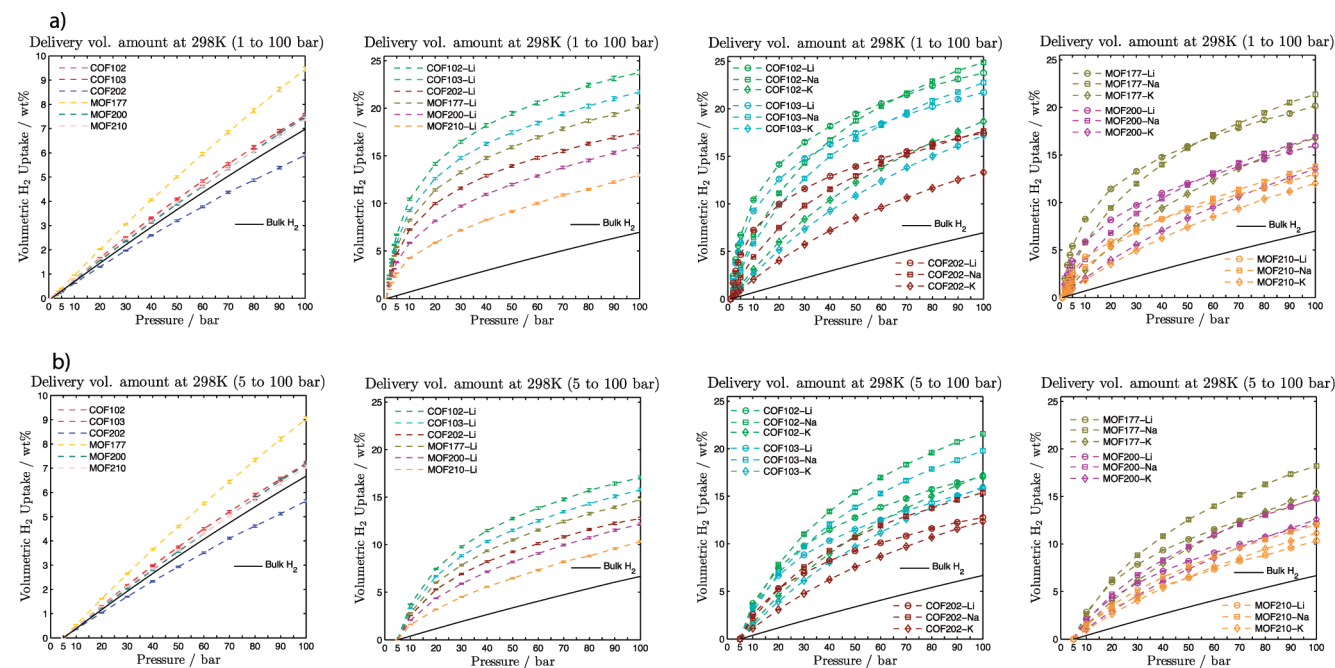
A possible explanation for this behavior is shown in Figure 5, where we plot V<sub>p</sub> versus wt% delivery amount using 1 and 5 bar as the delivery basis for all COFs. For this figure, MOFs were omitted for clarity, but the following discussion also applies (see Figures S19 and S20). Figure 5a,b shows that performance at higher pressures depends on the basis used to estimate the delivery amount. We found that the gravimetric uptake depends generally in higher degree on the V<sub>p</sub> than on the SA (Figure S21 vs S22), the same was suggested independently for the H<sub>2</sub> uptake in zeolitic imidizolate frameworks.<sup>17</sup> We also observed that the pore volume decreases as the size of the metalated atoms increases. Thus, the V<sub>p</sub> is bigger for the pure framework > Li-metalated > Na-metalated > K-metalated.

Figure 6a shows that when using 1 bar as the basis, the Li-metalated COFs gives a better delivery uptake at every pressure (10, 30, 50, 80, and 100 bar). Thus, at every coordinate, the uptake is higher for the Li-cases, with the difference getting smaller at 100 bar.

Figure 6b shows the delivery uptake with 5 bar as the basis, where we can see that at 10 bar the Li cases barely exceed the Na cases, and at 30 bar and above, the Na-analogs overcome any other counterparts. The K cases start performing closer to the Na cases with increasing pressure, while performing almost as good as the Li cases at 100 bar. We conclude that at lower pressure (1–10 bar) the Li cases perform better because the slope of the curves (uptake vs V<sub>p</sub> at constant pressure) is larger than the others, while the slope of the Na cases starts becoming larger than the Li cases as the pressure increases above 30 bar. Finally, the



**Figure 5.** We show the correlation of Pore Volume ( $V_p$ ) vs wt% delivery for different COFs: pristine (dotted line), COF-Li (double dotted line), COF-Na (continuous line), and COF-K (dashed line). In (a) 1 bar is used as the basis, while in (b) 5 bar. Different colors represent different pressures.



**Figure 6.** Delivery volumetric uptake obtained for the pristine, Li-, Na-, and K-metalled COFs and MOFs are shown. In (a) we used 1 bar as the basis, while in (b) we used 5 bar as the basis. The error bars at each calculated point are shown, and in some cases, they are too small to fit inside the symbols. Bulk  $H_2$  is shown for comparison.

slope of the curves for the K cases starts becoming as large as the Na cases at 100 bar. In other words, the Li cases perform better in the range of 1–10 bar, while Na cases perform better in the range of 30–100 bar, and by extension, the K cases should perform better above 100 bar using 5 bar as the basis, all due to the dependence of their  $H_2$  affinity at different pressures. This explains why Na cases leads to better performance than the Li cases above 30 bar; the higher performance obtained from 1 to 10 for the Li cases is diminished by removing the uptake up to 5 bar

due to the basis. By extension, we can argue that the K cases will perform better than the Na cases above 100 bar.

We also calculated the excess gravimetric amount<sup>29,30</sup> in wt% at 298 K. In the case of the pristine frameworks (Figure S13) at 100 bar, we obtained the best performance for MOF177 with 0.87 excess wt%, followed by COF103 with 0.55 and MOF200 with 0.54. In our previous work, we compared the results from theory and experiment for different pristine MOFs and COFs to validate our methodology.<sup>10,11,16</sup>

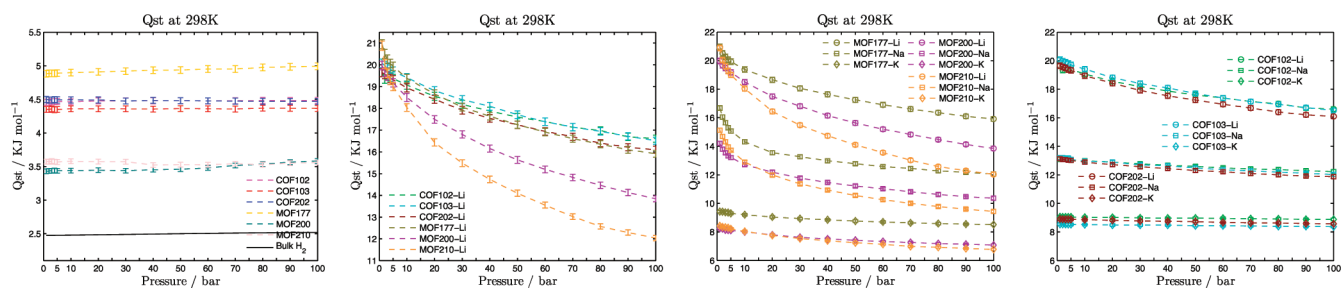


**Figure 7.** Heat of adsorption obtained for the pristine COFs and MOFs, as well as the analogs metalated with Li, Na, and K. MOF180 and MOF205 as well as the metalated cases are reported in the SI. Top plots show the error bars at each calculated point, and in the bottom plots, the error bars are too small that fit inside the symbols.

For the metalated compounds at 100 bar and 298 K (Figures S14 and S15), we obtained the best results for MOF200-Li, with 4.87 excess wt% units, followed by COF102-Li, with 4.84, and by COF103-Li, with 4.68. We found that for this pressure range the Li-metalated cases have a better performance than the Na analogs, which have better performance than the K-metalated frameworks. Using the same general principle given for delivery gravimetric units, but for this case the delivery basis is 0 bar, we expect the Na-based frameworks will eventually outperform the Li cases, but at a pressure beyond 100 bar, as Figures S14 and S15 suggest.

In a related work, we reported that IRMOF-2-96-Li reaches 5.6 excess wt% at 100 bar and 298 K,<sup>11</sup> while IRMOF-1-30-Li reaches 5.16 excess wt% at 100 bar and 298 K.<sup>10</sup> However, for application purposes, the delivery amount is the important unit because it determines the usable amount and here we have proven high excess amount uptake does not guarantee a high delivery amount at different basis.

**3.3. Volumetric Uptake.** We also calculated the *total*, *excess*, and *delivery* amount based on volumetric units (g H<sub>2</sub>/L) for all these compounds (Figure 6).

For the *delivery* volumetric amount, we found almost the same behavior as with delivery gravimetric units. When using the basis of 1 bar, the Na analogs overcome the Li analogs at pressures beyond 50 bar. The best performers at 100 bar and 298 K are COF102-Na with 24.9, followed by COF102-Li with 23.8, COF103-Na with 22.8, COF103-Li with 21.7, and MOF177-Na with 21.4, all using delivery g H<sub>2</sub>/L units.

On the other hand, when using the basis of 5 bar, the Na-based frameworks overcome the Li analogs at 20 bar. Also, the K-analogs overcome the Li-analogs at around 100 bar (at 60 bar in the case of MOF210) as we predicted it for the gravimetric uptake. At 100 bar and 298 K, we found the best performers are COF102-Na with 21.6, followed by COF103-Na with 19.8, MOF177-Na with 18.2, COF102-K with 17.2, and COF102-Li with 17.1, using delivery g H<sub>2</sub>/L units and basis equal to 5 bar.

For the *excess* volumetric amount (Figures S33–S35) at 100 bar and 298 K, we found the best performers are COF102-Na with 23.3, followed by COF102-Li with 22.2, then COF103-Na with 20.6, COF103-Li with 19.8 and MOF177-Na with 19.5, with excess g H<sub>2</sub>/L units. This is the same trend as the volumetric delivery amount using 1 bar as the basis. These new frameworks perform better than the best previously reported materials; MOF-C16-Li<sup>10</sup> (or IRMOF-1-16-Li) at 100 bar and 300 K reaches 17.3 excess g H<sub>2</sub>/L, while IRMOF-2-54-Li<sup>16</sup> reaches 19.2 excess g H<sub>2</sub>/L at the same thermodynamic conditions.

None of these compounds reach the volumetric 2010 DOE target of 28 g H<sub>2</sub>/L, but the closest compounds to this quantity are COF102-Na and COF103-Na with 24.9 and 22.8 delivery g H<sub>2</sub>/L from 1 to 100 bar (while 21.6 and 19.8 delivery g H<sub>2</sub>/L from 5 to 100 bar) at 298 K, respectively. These are to the best of our knowledge the highest molecular hydrogen uptake for a porous material in volumetric units under these thermodynamic conditions. Therefore, if a high delivery volumetric uptake is to be targeted, these results still suggest that high SA and V<sub>p</sub> are both important, where it should be remembered if V<sub>p</sub> is too large it could lead to a waste of space. Current analyzed COFs composed mainly of aromatic rings (COF102 and COF103) perform better in volumetric units than analyzed MOFs because for the former most of the atoms are accessible to interact with H<sub>2</sub>. In contrast, these MOFs with Zn clusters in their structures have zinc and oxygen atoms that are partially inaccessible (see inset of Figure 1). Also, a special case is COF202, where the *t*-butyl group used in the formation of the borosilicate has four carbons and one silicon atom per cab group that are partially unreachable as well (see Figure 1). This is, the more partially or totally inaccessible atoms the framework has, the worst performance in volumetric units, because these atoms that occupy space are not used to interact with H<sub>2</sub>.

**3.4. Isosteric Heat of Adsorption.** We also calculated the isosteric heat of adsorption (Qst) of these systems at 298 K. The unmetalated systems remain flat around 3.5–5 kJ/mol, while the Li-metalated cases vary from 13 to 21 kJ/mol, the Na-metalated cases are between 10 and 17 kJ/mol, and K-metalated frameworks window corresponds to 8–10 kJ/mol (see Figure 7). From these results we observe that a flat curve of Qst with high absolute value is better for the delivery amount (this is of course aside from the ideal Qst curve of increasing interaction at higher pressure). This is because for the delivery amount we do not want strong interaction energy at low pressure (below 1 or 5 bar), because this will bind a large number of molecules that will be difficult to remove after a cycle. For example, when discharging from 100 to 1 bar, the molecules absorbed from 0 to 1 bar will not be used. This can be seen in the Li cases, where they have the highest total uptake amount, but when we analyzed delivery units, they were overcome by the Na cases, which have a flatter Qst curve. The K cases have a flatter curve than the Na analogs; however, the absolute Qst value for Na cases is higher, therefore, they perform better than K-based frameworks at a pressure below 100 bar. This is another explanation for why the Na cases perform better at these delivery pressure ranges; Li cases bind too strongly to molecular hydrogen at lower pressure, while Na cases bind softer, resulting in a higher delivery amount.

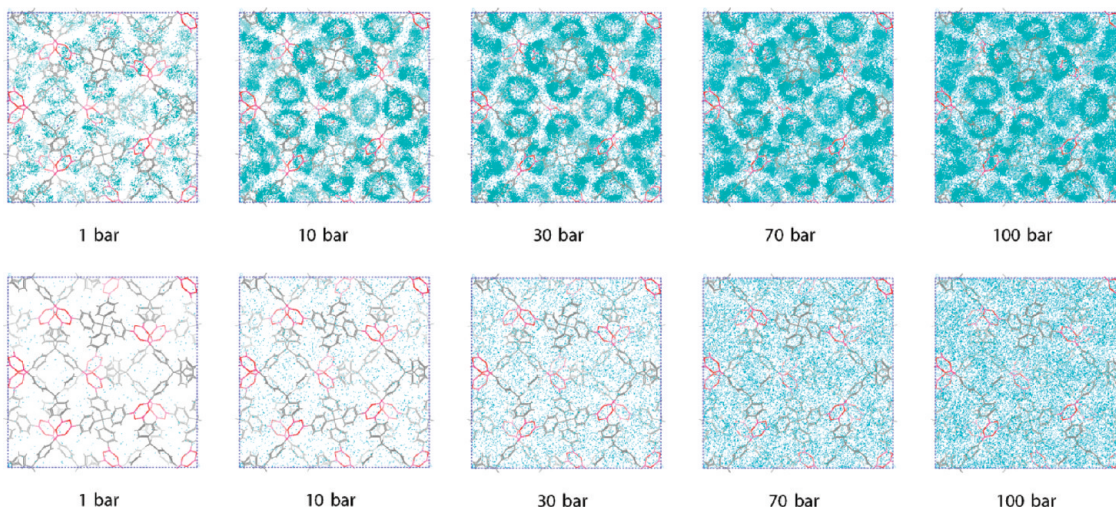


**Figure 8.** We show the ensemble average of molecular hydrogen for COF102 (bottom) and COF102-Li (top) at 298 K. Atom colors are C, gray; O, red; and B, pink; the average of molecular hydrogen is shown in green. COF103 and COF103-Li have the same mechanism as COF102 and COF102-Li, and they are not shown.

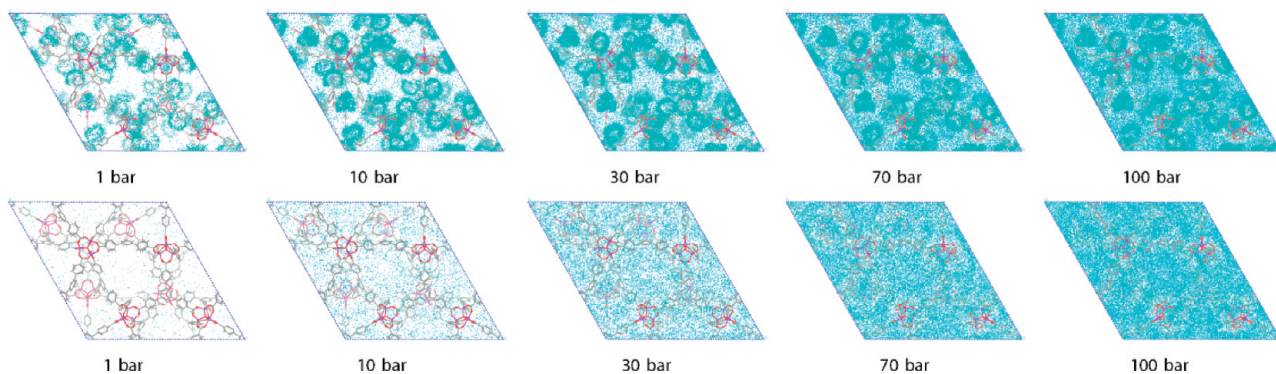


**Figure 9.** We show the ensemble average of molecular hydrogen for MOF177 (bottom) and MOF177-Li (top) at 298 K. Atoms colors are Zn, purple; C, gray; O, red; and the average of molecular hydrogen is shown in green. MOF200, MOF180, and MOF210 have a similar mechanism to MOF177 and they are not shown; the same applies to their metalated analogs.

While K cases have a flatter surface, which is optimal for charge/discharge purposes, its absolute value is too low to compete with the Na cases. Therefore, this study suggests that the next generation of frameworks targeting hydrogen adsorption with high delivery amount should have a flatter  $Q_{st}$ , and the absolute value should be at least as high as 15 kJ to reach the DOE gravimetric targets.

**3.5. Adsorption Mechanism of Molecular Hydrogen.** The multiple configurations that the  $\text{H}_2$  framework needs to explore at room temperature in the sorption process prompt us to analyze the mechanism from the ensemble average rather than single snapshots (Figures 8–10). After averaging the ensemble of all configurations, we found that the single layer mechanism is predominant for the metalated frameworks, while the pore filling mechanism appears after the sites surrounding the alkaline metals have been covered. On the other hand, for pristine COFs and MOFs, the pore filling mechanism is predominant, while there are not clear evidence about the formation of single layers. Previous works on the topic did not address the problem of the mechanism of hydrogen adsorption at room temperature; however, it is important to discern if there is a characteristic mechanism because it provides a validation for which physical

model can be used to represent each sorption curve. In this case, we have proved at the atomistic level, we can use the Langmuir model for metalated frameworks, while the BET model can be applied for pristine compounds both at low saturation uptakes. Although the connectivity and the topology of all these frameworks differ, the profile of the sorption at different pressures remains similar in all of them.

**3.6. Comparisons to Previous Computational Studies.** Subsequent to our work showing the Li-doped MOFs could lead to substantial  $\text{H}_2$  adsorption at room temperature,<sup>10</sup> Blomqvist et al.<sup>31</sup> used the generalized gradient approximation to density functional theory by using the projector augmented wave (PAW) method to confirm our results for Li-MOF5. However, if it is assumed that two Li atoms per benzene ring could be stable (one in each face), then a corrected DFT functional for vdW interactions should be used such as M06, because a function such as B3LYP would predict otherwise (Figure 2). Recently, Cao et al.<sup>32</sup> reported the uptake on COF102-Li and COF103-Li using force field parameters obtained from DFT/PW91. However, it is well-known that this level of DFT does not account for the London dispersion,

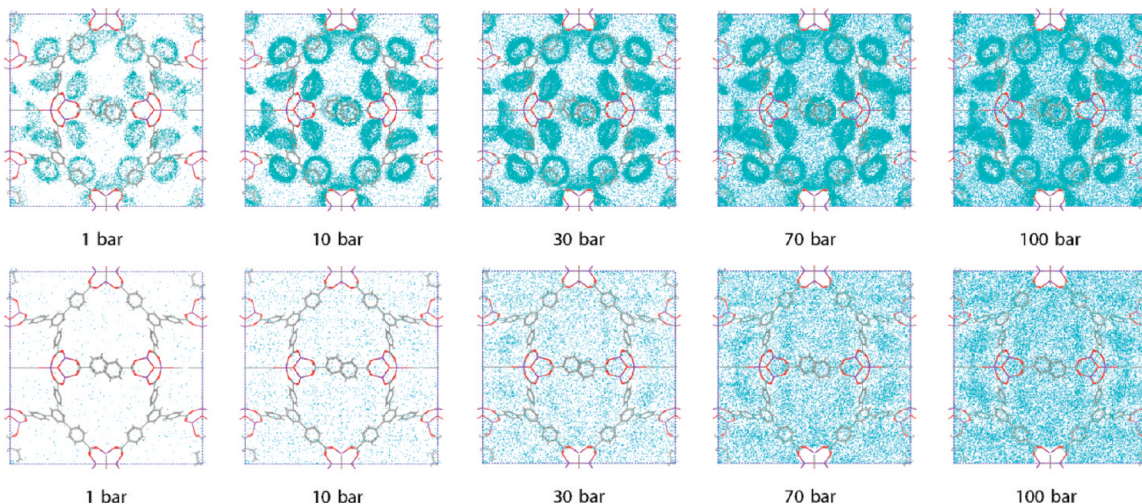


**Figure 10.** We show the ensemble average of molecular hydrogen for MOF205 (bottom) and MOF205-Li (top) at 298 K. Atom colors are the same as Figure 9.

so these results likely underestimate the reversible binding.<sup>12,33</sup> Therefore, these FF parameters have a lower quality than our CCSD(T) and MP2 calculations to estimate the dispersion interactions. This probably explains why they find a lower value for COF102-Li, with 4.25 effective wt% uptake, while from our calculation, we obtain 4.42 effective wt% (what is called in the literature effective amount<sup>34</sup> is what they define as excess amount), even though they report two Li atoms per benzene-BO<sub>2</sub> unit, while we report only one.

#### 4. CONCLUDING REMARKS

We have calculated the gravimetric and volumetric uptake for the latest generation of COFs and MOF, as well as their Li-, Na-, and K-metallated analogs. We also calculated the thermodynamics for the formation of the Li–Bz adduct and found that its formation is favorable when THF is used.

We found that for the gravimetric delivery amount from 1 to 100 bar, eleven compounds reach the 2010 DOE target of 4.5 wt %, while only two compounds reach the 2015 DOE target of 5.5 wt % (MOF200-Li and MOF200-Na).

However, none of these compounds reach the volumetric 2010 DOE target of 28 g H<sub>2</sub>/L, but the closest compound to this quantity is COF102-Na, with 24.9 delivery g H<sub>2</sub>/L. In general, an increase in porosity (or pore volume) of MOFs or COFs leads to an increase in the gravimetric H<sub>2</sub> uptake but decrease in the volumetric H<sub>2</sub> uptake. This can be seen when comparing MOF-200 and COF-102. The best gravimetric H<sub>2</sub> uptake is found in MOF-200 analogs, where pore volume is larger than any other MOFs and COFs considered here; however, the best volumetric H<sub>2</sub> uptake is found in the COF-102 analogs, which have one of the smallest pore volumes. Therefore, to increase volumetric uptake, it is better to consider MOFs or COFs with low pore volume (of around 1.8, but smaller than 2 cm<sup>3</sup> g<sup>-1</sup>) at the expense of reducing the gravimetric uptake.

In summary, we recommend three ways to improve both gravimetric and volumetric delivery units: (a) by creating compounds with high SA with all the atoms to be accessible, (b) by controlling the V<sub>p</sub> to get the best compromise of used space (smaller V<sub>p</sub> leads to better volumetric delivery, while bigger V<sub>p</sub> leads to a better gravimetric delivery), and (c) by aiming for a flat

Q<sub>st</sub> curve, which can be obtained when several strong sorption sites exist. According to the present work, a constant Q<sub>st</sub> value at least 15 kJ/mol should be obtained in order to reach the DOE gravimetric goal.

#### ■ ASSOCIATED CONTENT

**S Supporting Information.** The uptake for all metallated and pure MOFs and COFs is described. Sorption mechanism for the remaining COFs and MOFs is included. The new DOE targets for hydrogen storage updated on February 2009 are attached. This material is available free of charge via the Internet at <http://pubs.acs.org>.

#### ■ AUTHOR INFORMATION

##### Corresponding Author

\*E-mail: wag@wag.caltech.edu.

#### ■ ACKNOWLEDGMENT

J.L.M.-C. would like to acknowledge the Roberto Rocca Fellowship for support and Robert Nielsen for helpful discussions. S.S.H. acknowledges that this research was partially performed for the Hydrogen Energy R&D Center, one of the 21st Century Frontier R&D programs, funded by the Ministry of Education, Science and Technology of Korea. We thank Professor Omar Yaghi (UCLA) and Dr. Hiroyasu Furukawa (UCLA) for helpful discussions. W.A.G. and J.L.M.-C. acknowledge the DOE (DE-F6-36-08G018141, Program Manager Rich Bechtold) for supporting this research.

#### ■ REFERENCES

- (1) USDOE, Office of Energy Efficiency and Renewable Energy, The FreedomCAR and Fuel Partnership, Targets for Onboard Hydrogen Storage Systems for Light-Duty Vehicles, [https://www1.eere.energy.gov/hydrogenandfuelcells/storage/pdfs/targets\\_onboard\\_hydro\\_storage\\_explanation.pdf](https://www1.eere.energy.gov/hydrogenandfuelcells/storage/pdfs/targets_onboard_hydro_storage_explanation.pdf), 2009.
- (2) USDOE; USCAR; Shell; BP; ConocoPhillips; Chevron; ExxonMobil, The FreedomCAR and Fuel Partnership, Multi-Year Research,

Development and Demonstration Plan, <http://www1.eere.energy.gov/hydrogenandfuelcells/mypp/pdfs/storage.pdf>, 2009.

- (3) Han, S. S.; Mendoza-Cortes, J. L.; Goddard, W. A. *Chem. Soc. Rev.* **2009**, *38*, 1460–1476.
- (4) Cote, A. P.; Benin, A. I.; Ockwig, N. W.; O'Keeffe, M.; Matzger, A. J.; Yaghi, O. M. *Science* **2005**, *310*, 1166–1170.
- (5) El-Kaderi, H. M.; Hunt, J. R.; Mendoza-Cortes, J. L.; Cote, A. P.; Taylor, R. E.; O'Keeffe, M.; Yaghi, O. M. *Science* **2007**, *316*, 268–272.
- (6) Hunt, J. R.; Doonan, C. J.; LeVangie, J. D.; Cote, A. P.; Yaghi, O. M. *J. Am. Chem. Soc.* **2008**, *130*, 11872–11873.
- (7) Li, H.; Eddaoudi, M.; O'Keeffe, M.; Yaghi, O. M. *Nature* **1999**, *402*, 276–279.
- (8) Chae, H. K.; Siberio-Perez, D. Y.; Kim, J.; Go, Y.; Eddaoudi, M.; Matzger, A. J.; O'Keeffe, M.; Yaghi, O. M. *Nature* **2004**, *427*, 523–527.
- (9) Furukawa, H.; Ko, N.; Go, Y. B.; Aratani, N.; Choi, S. B.; Choi, E.; Yazaydin, A. O.; Snurr, R. Q.; O'Keeffe, M.; Kim, J.; Yaghi, O. M. *Science* **2010**, *329*, 424–428.
- (10) Han, S. S.; Goddard, W. A. *J. Am. Chem. Soc.* **2007**, *129*, 8422–8423.
- (11) Han, S. S.; Goddard, W. A. *J. Phys. Chem. C* **2008**, *112*, 13431–13436.
- (12) Zhao, Y.; Truhlar, D. G. *Acc. Chem. Res.* **2008**, *41*, 157–167.
- (13) Jaguar, version 7.6; Schrödinger, LLC, New York, NY, 2011.
- (14) Hart, J. R.; Rappe, A. K. *J. Chem. Phys.* **1992**, *97*, 1109–1115.
- (15) Hayes, J. M.; Greer, J. C.; Morton-Blake, D. A. *J. Comput. Chem.* **2004**, *25*, 1953–1966.
- (16) Han, S. S.; Furukawa, H.; Yaghi, O. M.; Goddard, W. A. *J. Am. Chem. Soc.* **2008**, *130*, 11580–11581.
- (17) Han, S. S.; Choi, S. H.; Goddard, W. A. *J. Phys. Chem. C* **2011**, *115*, 3507–3512.
- (18) Mayo, S. L.; Olafson, B. D.; Goddard, W. A. *J. Phys. Chem.* **1990**, *94*, 8897–8909.
- (19) Bae, Y. S.; Lee, C. H. *Carbon* **2005**, *43*, 95–107.
- (20) Becke, A. D. *J. Chem. Phys.* **1993**, *98*, 5648–5652.
- (21) Lee, C. T.; Yang, W. T.; Parr, R. G. *Phys. Rev. B* **1988**, *37*, 785–789.
- (22) Tannor, D. J.; Marten, B.; Murphy, R.; Friesner, R. A.; Sitkoff, D.; Nicholls, A.; Ringnalda, M.; Goddard, W. A.; Honig, B. *J. Am. Chem. Soc.* **1994**, *116*, 11875–11882.
- (23) Tacke, M. *Chem. Ber.* **1996**, *129*, 1369–1371.
- (24) Tacke, M. *Eur. J. Inorg. Chem.* **1998**, 537–541.
- (25) Krieck, S.; Gorls, H.; Westerhausen, M. *Organometallics* **2010**, *29*, 6790–6800.
- (26) Nelson, A. P.; Farha, O. K.; Mulfort, K. L.; Hupp, J. T. *J. Am. Chem. Soc.* **2009**, *131*, 458–460.
- (27) Biloe, S.; Goetz, V.; Mauran, S. *AIChE J.* **2001**, *47*, 2819–2830.
- (28) Lozano-Castello, D.; Alcaniz-Monge, J.; de la Casa-Lillo, M. A.; Cazorla-Amoros, D.; Linares-Solano, A. *Fuel* **2002**, *81*, 1777–1803.
- (29) Furukawa, H.; Miller, M. A.; Yaghi, O. M. *J. Mater. Chem.* **2007**, *17*, 3197–3204.
- (30) Excess Uptake: In sorption experiments the excess amount is obtained but the absolute amount can only be estimated. The absolute adsorbed amount can be estimated from experimental data by using  $N_{\text{total}} = N_{\text{excess}} + V_p \times \text{density}(\text{bulk})$ , where  $N_{\text{excess}}$  is the excess mass  $V_p$  is the pore volume  $N_{\text{total}}$  is total adsorbed amount of molecular hydrogen. Density (bulk) is the bulk density of molecular hydrogen. However, from our GCMC calculations, we obtain  $N_{\text{total}}$  directly.
- (31) Blomqvist, A.; Araujo, C. M.; Srepusharawoot, P.; Ahuja, R. *Proc. Natl. Acad. Sci. U.S.A.* **2007**, *104*, 20173–20176.
- (32) Cao, D. P.; Lan, J. H.; Wang, W. C.; Smit, B. *Angew. Chem., Int. Ed.* **2009**, *48*, 4730–4733.
- (33) Zhao, Y.; Schultz, N. E.; Truhlar, D. G. *J. Chem. Theory Comput.* **2006**, *2*, 364–382.
- (34) Zhou, W.; Wu, H.; Hartman, M. R.; Yildirim, T. *J. Phys. Chem. C* **2007**, *111*, 16131–16137.
- (35) Boys, S. F.; Bernardi, F. *Mol. Phys.* **1970**, *19*, 553–&.